



## Transport Phenomena in Polymer Electrolyte Membranes

### II. Binary Friction Membrane Model

J. Fimrite, B. Carnes, H. Struchtrup, and N. Djilali<sup>z</sup>

Institute for Integrated Energy Systems, University of Victoria, Victoria,  
British Columbia, Canada V8W 3P6

The insight gained from the analysis conducted in Part I (see the preceding article) is used in the development of a general transport model for water and protons in perfluorosulfonic acid membranes based on the binary friction model. As a tool for investigating the unknown parameters in the general membrane transport model, a simplified conductivity model is derived to represent conditions found in alternating current (ac) impedance conductivity measurements. This binary friction conductivity model (BFCM) is applied to 1100 equivalent weight (EW) Nafion, and compared to other established membrane models. It is shown to provide a more consistent fit to the data over the entire range of water contents and at different temperatures. The subset of transport coefficients in the BFCM is the same as in the general binary friction membrane model (BFM2), and with additional data on water transport, the BFM2 model and all its required parameters can be fully specified. The paper discusses possible experimental investigations and fundamental simulations to determine the model parameters required to apply the general BFM2 to predict coupled proton and water transport in PEM fuel cells.

© 2005 The Electrochemical Society. [DOI: 10.1149/1.1952647] All rights reserved.

Manuscript submitted July 28, 2004; revised manuscript received April 18, 2005. Available electronically July 25, 2005.

This work is motivated by the need for improved and more general models to represent transport phenomena within polymer electrolyte membranes. Such models are essential to support ongoing development of computational fuel cell dynamic models required for fundamental simulation of in situ processes that are difficult to observe experimentally, as well as for design and optimization.

In Part I of this work,<sup>1</sup> we examined various macroscopic membrane transport models proposed to date, and resolved a fundamental formulation issue by showing that the binary friction model (BFM) provides a physically consistent modeling framework, and implicitly accounts for viscous transport. In this second part, we focus on the use of this framework to develop a new binary friction membrane transport model (BFM2) which

1. Relies on rationally derived transport equations based on the physics of multicomponent transport in the membrane.
2. Removes the redundant viscous terms.
3. Is not restricted by the assumption of equimolar counter diffusion.<sup>2</sup>
4. Accounts for the effect of temperature on the sorption isotherm.

Following the derivation of the BFM2, and in order to gain insight and prescribe the unknown transport parameters, we simplify the model in the limit of a uniformly hydrated membrane to match the conditions of ac impedance conductivity measurements. Using empirically fitted transport parameters, the predictive ability of the model is then assessed for Nafion 1100 equivalent weight (EW) membranes. The paper closes with some discussion on required additional data for applying the model to other perfluorosulfonic acid (PFSA) membranes.

#### Binary Friction Membrane Model

*General model.*—The binary friction model (BFM) for the general case of  $n$  species diffusing in a porous medium is defined by<sup>1,2</sup>

$$-\frac{1}{RT}\nabla_T\mu_i^e = \sum_{j=1}^n \frac{X_j}{D_{ij}^e} \left( \frac{N_i}{c_i} - \frac{N_j}{c_j} \right) + \frac{1}{D_{iM}^e} \left( \frac{N_i}{c_i} \right), \quad i = 1, \dots, n \quad [1]$$

In the above equation  $\mu_i^e$  is the electrochemical potential of species  $i$ ,  $D_{ij}^e$  is the *effective* Stefan-Maxwell binary diffusion coefficient between species  $i$  and  $j$ , and  $D_{iM}^e$  is the effective diffusion coefficient between species  $i$  and the porous medium. Physically, the  $D_{ij}^e$  relate

changes in *relative* species fluxes to gradients in the electrochemical composition of the mixture arising from species-species interactions, while the  $D_{iM}^e$  relate *absolute* species fluxes to gradients in individual electrochemical potential gradients, arising from species-medium interactions, the so-called Knudsen diffusion effect.

The effective binary diffusion coefficients are defined by scaling the standard binary diffusion coefficients using the porosity  $\varepsilon$  and tortuosity factor  $\tau$  according to

$$D_{ij}^e = \frac{\varepsilon}{\tau} D_{ij} \quad [2]$$

The effective diffusion coefficients  $D_{iM}^e$  between the species and porous medium are assumed to follow the same scaling for appropriate reference values  $D_{iM}$ . An alternative to the above correction that avoids the use of the tortuosity is the Bruggeman correction<sup>3</sup>

$$D_{ij}^e = (\varepsilon - \varepsilon_0)^q D_{ij} \quad [3]$$

where  $\varepsilon_0$  is the threshold porosity, which is the minimum fraction of the volume that must be occupied by the fluid to allow transport. The Bruggeman exponent  $q$  is either used as a fitted parameter or is given the value of 1.5.

Using a standard derivation, the gradient in electrochemical potential (at constant temperature  $T$ ) can be expressed as<sup>a</sup>

$$\nabla_T\mu_i^e = RT(\nabla \ln X_i + \nabla \ln \gamma_i) + V_{M,i} \nabla p + z_i F \nabla \Phi \quad [4]$$

where the terms represent the effects of composition, activity, Gibb's free energy, and electrical potential.  $X_i$  is the mole fraction,  $\gamma_i$  is the activity,  $V_{M,i}$  is the specific molar volume,  $z_i$  is the charge, and  $\Phi$  is the ionic potential. Introducing the above definition of the gradient of the electrochemical potential into the BFM (Eq. 1) and multiplying both sides by the mole fraction  $X_i$ , we obtain

$$-\left( \nabla X_i + X_i \nabla \ln \gamma_i + X_i \frac{V_{M,i}}{RT} \nabla p + X_i z_i \frac{F}{RT} \nabla \Phi \right) = \sum_{j=1}^n \left\{ \frac{X_j N_i}{c_i D_{ij}^e} - \frac{X_i N_j}{c_j D_{ij}^e} \right\} + \frac{N_i}{c_i D_{iM}^e}, \quad i = 1, \dots, n \quad [5]$$

*Specialization of BFM to a PEM.*—We consider transport within the family of perfluorosulfonic acid (PFSA) membranes, such

<sup>a</sup>Note that this expression for electrochemical potential is different from that in other studies, e.g., Thampan et al. (Ref. 2), in that mole fractions are used here instead of molar densities and molar volumes instead of partial molar volumes. This difference arises because a different reference state was chosen in the development of the chemical potential terms.

<sup>z</sup> E-mail: ndjilali@uvic.ca

**Table I. Nondimensional quantities and associated reference values.**

Nondimensional quantities		Reference values
Length	$\hat{x} = x/L_M$	$L_M = \text{membrane thickness}$
Total mole density	$\hat{c}_t = c_t/c_{\text{ref}}$	$c_{\text{ref}} = 1/V_{M2} = 55.6 \times 10^{-3} \text{ mol m}^{-3}$
Mole density of species $i$	$\hat{c}_i = c_i/c_{\text{ref}}$	$c_{\text{ref}} = 1/V_{M2} = 55.6 \times 10^{-3} \text{ mol m}^{-3}$
Mole flux	$\hat{N}_i' = N_i'/N_{\text{ref}}$	$N_{\text{ref}} = c_{\text{ref}}v_{\text{ref}}, v_{\text{ref}} = D_{\text{ref}}/L_M$
Molar volume	$\hat{v}_1 \approx \hat{v}_2 = V_{M,2}/V_{M,\text{ref}}$	$V_{M,\text{ref}} = 1/c_{\text{ref}} = V_{M,2}$
Diffusion coefficients	$\hat{D}_{ij} = D_{ij}^{S-M}/D_{\text{ref}}, \hat{D}_{ij}^e = D_{ij}^e/D_{\text{ref}}$	$D_{\text{ref}} = D_{ij}^{S-M}, \text{ or } D_{\text{im}}^e$
Pressure gradients	$\hat{\nabla} \hat{p} = \nabla p / (\Delta p_{\text{ref}}/L_M)$	$\Delta p_{\text{ref}} = 5 \times 10^5 \text{ N m}^{-2}$
Potential gradients	$\hat{\nabla} \hat{\Phi} = \nabla \Phi / (\Delta \Phi_{\text{ref}}/L_M)$	$\Delta \Phi_{\text{ref}} = 0.3 \text{ V}$
Gradient operator	$\hat{\nabla} = L_m \nabla$	$L_M = \text{membrane thickness}$
Additional coefficients	$\beta = \Delta p_{\text{ref}}/RTc_{\text{ref}}$ $\Theta = F\Delta \Phi_{\text{ref}}/RT$	$c_{\text{ref}} = 1/V_{M,2} = 55.6 \times 10^{-3} \text{ mol m}^{-3}, \Delta p_{\text{ref}} = 5 \times 10^5 \text{ N m}^{-2}$ $c_{\text{ref}} = 1/V_{M,2} = 55.6 \times 10^{-3} \text{ mol m}^{-3}, \Delta \Phi_{\text{ref}} = 0.3 \text{ V}$

as Nafion. The membrane is taken as the porous medium, and only two species are assumed present in the pore fluid, proton carriers (species  $i = 1$ ) and water ( $i = 2$ ). Furthermore, we assume that the dominant proton carrier is hydronium.

In order to identify terms that may be neglected to simplify the numerical solution and to improve physical insight, the system in Eq. 6 is nondimensionalized using the parameters and variables found in Table I

$$\begin{aligned}
 & -(\hat{\nabla} X_i + X_i \hat{\nabla} \ln \gamma_i + \beta X_i \hat{v}_i \hat{\nabla} \hat{p} + \Theta X_{i,z_i} \hat{\nabla} \hat{\Phi}) \\
 & = \sum_{j=1}^2 \left\{ \frac{X_j \hat{N}_i}{\hat{c}_t \hat{D}_{ij}} - \frac{X_i \hat{N}_j}{\hat{c}_t \hat{D}_{ij}} \right\} + \frac{\hat{N}_i}{\hat{c}_t \hat{D}_{iM}} \quad i = 1, 2 \quad [6]
 \end{aligned}$$

The reference molar densities are chosen to be the inverse of the partial molar volume of water, because this does not vary significantly with temperature or pressure. We assume the molar volumes for water and hydronium to be the same (see the Appendix). To perform an order of magnitude analysis of the driving force terms, we assume, as a limiting case scenario, the pressure drop across the membrane to be 5 bar, thus  $\Delta p_{\text{ref}} = 5 \times 10^5 \text{ N m}^{-2}$ , while the maximum potential drop across the membrane is approximately 0.3 V, and  $\Delta \Phi_{\text{ref}} = 0.3 \text{ V}$ .

Following previous studies,<sup>2</sup> we assume the gradients in composition are small and, thus, gradients in the activity coefficients are negligible, i.e. ( $X_i \hat{\nabla} \ln \gamma_i \cong 0$ ).

*Magnitude of the coefficients for the driving force terms.*—Using the values in Table I, the coefficients for the driving force terms are estimated in Table II. Compared to the potential and mole fraction gradient terms, the pressure terms are of a significantly lower order and can be neglected. Also, the potential term is the dominant term when  $z_i \neq 0$ , while the gradient in mole fraction term is dominant when  $z_i = 0$ .

Considering Eq. 6, and simplifying according to the assumptions made in the previous section, we arrive at

**Table II. Comparing the relative magnitude of the driving forces in the transport equations.**

Gradient of interest	Coefficient for gradient term	Coefficient value	Approximate order of magnitude
$\hat{\nabla} X_1, \hat{\nabla} X_2$	1	1	$\sim 1$
$\hat{\nabla} \hat{p}$	$X_1 \hat{v}_1 \beta$	$X_1 (3.15 \times 10^{-3})$	$\sim 10^{-3}$
	$X_2 \hat{v}_2 \beta$	$X_2 (3.15 \times 10^{-3})$	$\sim 10^{-3}$
$\hat{\nabla} \hat{\Phi}$	$X_1 \Theta$	$X_1 (10.1)$	1-10

$$-(\hat{\nabla} X_i + \Theta X_{i,z_i} \hat{\nabla} \hat{\Phi}) = \sum_{j=1}^n \left\{ \frac{X_j \hat{N}_i}{\hat{c}_t \hat{D}_{ij}} - \frac{X_i \hat{N}_j}{\hat{c}_t \hat{D}_{ij}} \right\} + \frac{\hat{N}_i}{\hat{c}_t \hat{D}_{iM}} \quad i = 1, 2 \quad [7]$$

Expanding this for both species ( $i = 1, 2$ )

$$-(\hat{\nabla} X_1 + \Theta X_1 \hat{\nabla} \hat{\Phi}) = \left\{ \frac{X_2 \hat{N}_1}{\hat{c}_t \hat{D}_{12}} - \frac{X_1 \hat{N}_2}{\hat{c}_t \hat{D}_{12}} \right\} + \frac{\hat{N}_1}{\hat{c}_t \hat{D}_{1M}} \quad [8]$$

$$-(\hat{\nabla} X_2) = \left\{ \frac{X_1 \hat{N}_2}{\hat{c}_t \hat{D}_{12}} - \frac{X_2 \hat{N}_1}{\hat{c}_t \hat{D}_{12}} \right\} + \frac{\hat{N}_2}{\hat{c}_t \hat{D}_{2M}} \quad [9]$$

For species 2, we invoke the property of the BFM that<sup>4</sup>  $\hat{D}_{ij} = \hat{D}_{ji}$ .

Casting the above into matrix form, and inverting the matrix to obtain an expression for the fluxes in terms of the driving forces yields

$$\begin{pmatrix} \hat{N}_1 \\ \hat{N}_2 \end{pmatrix} = -\frac{\hat{c}}{\chi} \begin{bmatrix} \left( \frac{X_1}{\hat{D}_{12}} + \frac{1}{\hat{D}_{2M}} \right) & \frac{X_1}{\hat{D}_{12}} \\ \frac{X_2}{\hat{D}_{12}} & \left( \frac{X_2}{\hat{D}_{12}} + \frac{1}{\hat{D}_{1M}} \right) \end{bmatrix} \begin{pmatrix} \hat{\nabla} X_1 + \Theta X_1 \hat{\nabla} \hat{\Phi} \\ \hat{\nabla} X_2 \end{pmatrix} \quad [10]$$

where  $\chi$  is the determinant

$$\chi = \frac{X_1}{\hat{D}_{12} \hat{D}_{1M}} + \frac{X_2}{\hat{D}_{12} \hat{D}_{2M}} + \frac{1}{\hat{D}_{1M}^e \hat{D}_{2M}}$$

*Dissociation model.*—In order to develop expressions for the mole fractions  $X_i$  in terms of the membrane water content  $\lambda$ , we introduce the degree of dissociation  $\alpha$ , which can be determined by using the thermodynamic equilibrium model of Thampan et al.<sup>2</sup>

$$\alpha = \frac{(\lambda + 1) - \sqrt{(\lambda + 1)^2 - 4\lambda \left( 1 - \frac{1}{K_{A,C}} \right)}}{2 \left( 1 - \frac{1}{K_{A,C}} \right)} \quad [11]$$

where  $K_{A,C}$  is the equilibrium constant for proton solvation in terms of mole densities

$$K_{A,C} = K_{A,C,298} \exp \left[ -\frac{\Delta H^0}{R} \left( \frac{1}{T} - \frac{1}{298} \right) \right] \quad [12]$$

and

$$\Delta H^0 = -52.3 \text{ kJ/mol}$$

$$K_{A,C,298} = 6.2 \quad [13]$$

A plot of the degree of dissociation using Eq. 11 shows that the first two waters sorbed by the membrane ( $\lambda = 2$ ) cause a significant portion of the protons to dissociate from the sulfonate heads to form hydronium ions.

**BFM2 model.**—We now introduce our definitions of the mole fractions  $X_1$  and  $X_2$

$$X_1 = \frac{\alpha}{\lambda} \quad [14]$$

$$X_2 = \frac{\lambda - \alpha}{\lambda} \quad [15]$$

which are derived in the Appendix and satisfy  $X_1 + X_2 = 1$ . In the above expressions  $\alpha$  is the fraction of dissociated acid heads. Because both  $X_1$  and  $X_2$  are functions of  $\lambda$ , we also have

$$\hat{\nabla} X_1 = -\hat{\nabla} X_2 = \frac{\partial X_1}{\partial \lambda} \hat{\nabla} \lambda = \left\{ \begin{array}{c} -\alpha + \lambda \frac{\partial \alpha}{\partial \lambda} \\ -\frac{\alpha}{\lambda^2} \end{array} \right\} \hat{\nabla} \lambda \quad [16]$$

Introducing the above expressions for spatial mole fraction gradients and mole fractions into Eq. 10, we obtain

$$\begin{pmatrix} \hat{N}_1 \\ \hat{N}_2 \end{pmatrix} = \frac{-\hat{c}}{\lambda^2 \chi} \begin{bmatrix} \left( \frac{\alpha^2}{\hat{D}_{12}} + \frac{\alpha \lambda}{\hat{D}_{2M}} \right) \Theta & \left( \frac{-\alpha + \lambda \frac{\partial \alpha}{\partial \lambda}}{\hat{D}_{2M}} \right) \\ \left( \frac{\alpha(\lambda - \alpha)}{\hat{D}_{12}} \right) \Theta & \left( \frac{\alpha - \lambda \frac{\partial \alpha}{\partial \lambda}}{\hat{D}_{1M}} \right) \end{bmatrix} \begin{pmatrix} \hat{\nabla} \Phi \\ \hat{\nabla} \lambda \end{pmatrix} \quad [17]$$

$$\chi = \frac{1}{\lambda} \left( \frac{\alpha}{\hat{D}_{12} \hat{D}_{1M}} + \frac{(\lambda - \alpha)}{\hat{D}_{12} \hat{D}_{2M}} + \frac{\lambda}{\hat{D}_{1M} \hat{D}_{2M}} \right) \quad [18]$$

We also have an expression for the porosity  $\varepsilon$  as a function of water content

$$\varepsilon(\lambda) = \frac{\lambda}{\lambda + V_{M,M}/V_{M,2}} \quad [19]$$

which we develop in the Appendix. The threshold porosity  $\varepsilon_0$  in the Bruggeman correction (Eq. 3) is defined by specifying a minimum water content  $\lambda_{\min}$  with  $\varepsilon_0 = \varepsilon(\lambda_{\min})$ . Here,  $\lambda_{\min}$  is the minimum amount of water that must be sorbed by the membrane for the pore liquid phase to be sufficiently well connected to allow for transport through the membrane.

We now have a set of general equations describing transport within PFSA membranes. The model, however, contains a set of transport coefficients ( $D_{12}$ ,  $D_{1M}$ , and  $D_{2M}$ ) that needs to be specified for practical applications. In the absence of data in the literature, these coefficients can be determined using related transport properties measured under known conditions.

Conductivity is directly related to the transport of hydronium ions through the membrane, and is the best-documented transport property. In the next section we reduce the BFM2 model (Eq. 17-19) to a conductivity model. It should be emphasized that this conductivity model is derived here primarily as a tool to gain insight and prescribe the unknown transport coefficients.

### Binary Friction Conductivity Model

Conductivity measurements are commonly performed on membranes using an impedance measurement techniques.<sup>4</sup> In such experiments, it is reasonable to assume that the membrane is uniformly equilibrated with water vapor and thus that the gradient in water content is zero. It follows from Eq. 17 that the protonic flux is then

proportional to the potential gradient in the membrane. Applying this assumption to (Eq. 17), and reintroducing the determinant (Eq. 18), we have

$$\hat{N}'_1 = \frac{-\hat{c}}{\lambda} \frac{\frac{\alpha^2}{\hat{D}_{12}} + \frac{\alpha \lambda}{\hat{D}_{2M}}}{\frac{\alpha}{\hat{D}_{12} \hat{D}_{1M}} + \frac{\lambda - \alpha}{\hat{D}_{12} \hat{D}_{2M}} + \frac{\lambda}{\hat{D}_{1M} \hat{D}_{2M}}} \Theta \hat{\nabla} \Phi \quad [20]$$

The ionic current density is related to the ionic fluxes by Faraday's law

$$i = F \sum_{i=1}^2 z_i N_i = F N_1 \quad [21]$$

and conductivity is defined as

$$\sigma \equiv \frac{-i}{\nabla \Phi} \quad [22]$$

Using Eq. 20 and 21, reintroducing the dimensional quantities into Eq. 19, and recalling that we use the Bruggeman correction in Ref. 3, we obtain the binary friction conductivity model

$$\sigma = (\varepsilon - \varepsilon_0)^g \frac{c_t F^2}{RT \lambda} \frac{\frac{\alpha^2}{D_{12}} + \frac{\alpha \lambda}{D_{2M}}}{\frac{\alpha}{D_{12} D_{1M}} + \frac{\lambda - \alpha}{D_{12} D_{2M}} + \frac{\lambda}{D_{1M} D_{2M}}} \quad [23]$$

In order to apply this expression to determine conductivity,  $D_{12}$ ,  $D_{1M}$ , and  $D_{2M}$  need to be prescribed, and their value should be based on specific membrane characteristics and empirical data as discussed next.

At this juncture, two points should be emphasized:

1. Equation 23 is not equivalent to Eq. 17; it is merely a reduction of Eq. 17 in the limit of either negligible water content gradient in the membrane, or negligible upper off-diagonal term  $[-\alpha + \lambda(\partial \alpha / \partial \lambda)] / \hat{D}_{2M}$ . As such, and similarly to other established membrane models,<sup>2,5</sup> Eq. 23 does not account for the impact of water flux on protonic current.

2. However, Eq. 23 has the useful property of containing the same transport coefficients as the general BFM2 (Eq. 17), and thus any appropriate choice of parameters for the BFCM automatically and conveniently defines a set of parameters for the more general BFM2. Therefore, with additional data on water transport, the BFM2 model, which does account for the coupling between protonic current and water flux, can be fully specified and applied.

### Functional Dependence of Diffusion Coefficients on Water Content ( $\lambda$ )

**Hydronium-water interaction ( $D_{12}$ ).**—We assume the interaction between water and hydronium ions does not depend on water content, which is reasonable based on studies of the Stefan-Maxwell coefficients for systems of nonideal fluids.<sup>6</sup> Furthermore, since  $D_{12}$  represents binary diffusion within the fluid in the membrane, it should not depend on the water content  $\lambda$ , except through the Bruggeman correction (Eq. 3).

**Species-membrane interactions ( $D_{1M}$  and  $D_{2M}$ ).**—In the absence of specific knowledge on species-membrane interaction, it is reasonable to assume the interaction depends on the water content due to changes in the geometry of the membrane, and the proximity of the species to the membrane. In order to determine the empirical fit of our model parameters based on conductivity data, we assumed a simple power-law dependence, so that both  $D_{1M}$  and  $D_{2M}$  are increasing functions of  $\lambda$  as

$$D_{1M} \propto \lambda^s \text{ and } D_{2M} \propto \lambda^s \quad [24]$$

**Table III. Parameters required for implementation of the BFCM.**

Parameter	Determination
$\alpha$ , fraction of dissociated acid heads	Eq. 11
$\varepsilon$ , porosity	Eq. A-13
$\varepsilon_0$ , threshold porosity	Empirical fit
$q$ , Bruggeman exponent	1.5, Ref. 2
$D_{12}$ , diffusion coefficient (hydronium - water)	Empirical fit
$D_{1M}$ , diffusion coefficient (hydronium - membrane)	Eq. 32, Empirical fit
$D_{2M}$ , diffusion coefficient (water - membrane)	Eq. 32, Empirical fit
$s$ , exponent for diffusion coefficients	Empirical fit

### Summary of Conductivity Model Development

The BFCM developed above (Eq. 23) results from simplifying the BFM2 (Eq. 17), according to the conditions of the ac impedance experiments used to measure conductivity. The primary objective of the next sections is to illustrate how, given a specific membrane and a set of experimental data, the BFCM can be used to prescribe the unknown model parameters (Table III) using constitutive relations, complementary models, or fitting to empirical conductivity data.

A model is available for the dissociation behavior (Eq. 11-13), a porosity function is included (Eq. 19), and the Bruggeman relation (see Eq. 3) is used with the value of  $q$  commonly taken to be<sup>2</sup> 1.5.

We assume that  $D_{12}$  does not depend on water content, and we have proposed a functional dependence of the diffusion coefficients  $D_{1M}$  and  $D_{2M}$  on water content (Eq. 24). The unknown parameters required in the model developed in the preceding section ( $D_{12}$ ,  $D_{1M}$  and  $D_{2M}$ ,  $\varepsilon_0$ , and  $s$ ) are estimated by fitting experimental data of Sone et al. at two temperatures, 30 and 70°C. Again, we emphasize that these parameters are identical for both the simplified conductivity model and the general binary friction membrane model. Once determined, these parameters can be reintroduced into the BFM2, and the model applied to compute coupled water and ionic transport, but this is beyond the scope of this work.

### Experimental Data

**Conductivity data.**—Sone et al.<sup>4</sup> reported conductivity data for Nafion 117 in the *E* form (no heat treatment), measured using a four-electrode ac impedance method. Membranes used in fuel cells are typically heated during the manufacture of the membrane electrode assembly, and it may thus be more appropriate to fit to the data for a membrane in the *N* or *S* form; however, fitting to the *E*-form data allows direct comparison with Thampan et al.'s<sup>2</sup> fit to their model.

Sone et al.'s data are measured in the plane of the membrane, but are expected to provide a reasonable measure of the normal direction conductivity because Nafion presents no apparent ordering of the macromolecules in any preferential direction, and its properties are expected to be reasonably isotropic. We also assume that the conductivity data measured by Sone and co-workers represent the conductivity of all 1100 EW Nafion membranes (all thicknesses).

In Ref. 4 the conductivity data (in S cm<sup>-1</sup>) collected were fitted to a third-degree polynomial, i.e.

$$\sigma_{\text{Sone}} = a_{\text{Sone}} + b_{\text{Sone}}x + c_{\text{Sone}}x^2 + d_{\text{Sone}}x^3 \quad [25]$$

where  $x$  is the relative humidity ( $x = 100 p/p_{\text{sat}}(T) = 100a$ ), and the coefficients ( $a_{\text{Sone}}$ ,  $b_{\text{Sone}}$ ,  $c_{\text{Sone}}$ , and  $d_{\text{Sone}}$ ) are given for various temperatures. We use the data for the *E* form of Nafion for 30 and 70°C. The data for 30°C are used to fit the parameters because the sorption isotherm data are available from a number of different sources at or near 30°C. The data at 70°C are used to investigate how the parameters vary with temperature. It is important to assess the model predictions at this temperature, because it is more representative of typical PEM fuel cell operating temperatures.

**Sorption isotherms.**—An added complication is that the conductivity data of Sone et al.<sup>4</sup> are given as a function of activity

[ $\sigma = \sigma(a)$ ] of the water vapor outside of the membrane with which the membrane is equilibrated. However, in the BFM2, as well as in the models of Springer et al.<sup>5</sup> and Thampan et al.,<sup>2</sup> conductivity is defined as a function of  $\lambda$ , which we recall is the number of water molecules sorbed within the membrane per sulfonate head. Casting conductivity as a function of  $\lambda$ , rather than activity, is more practical in applying the membrane model because  $\lambda$  is taken in general as varying throughout the membrane.

**Sorption isotherm fit at 30°C.**—To convert the data of Sone et al.<sup>4</sup> from a function of relative humidity  $x$  to a function of water content, we require the activity  $a$  as a function of water content  $\lambda$ . This is accomplished using a least-squares fit of a third-degree polynomial to fit the available sorption isotherm data from Sone et al.<sup>4</sup> at 30°C with  $\lambda$  as the independent variable and activity as the dependent variable. The resulting expression is

$$a_{30\text{C}} = b_0 + b_1\lambda + b_2\lambda^2 + b_3\lambda^3 \quad [26]$$

with coefficients

$$b_0 = -0.246, \quad b_1 = 0.232, \quad b_2 = -0.0147, \quad b_3 = 3.149 \times 10^{-4} \quad [27]$$

The largest standard error was found to be SE = 0.038 43, and was added or subtracted from the least-squares fit to estimate the error in our curve fit

$$a|_{\text{error}} = a_{30\text{C}} \pm \text{SE} \quad [28]$$

**Sorption isotherm fit at 80°C.**—We assume the data in Ref. 7 for 80°C are for a membrane with no heat treatment (*E* form), and applying a similar procedure on Nafion 117 data at 80°C, a fourth-order polynomial was fitted

$$a_{80\text{C}} = b_0 + b_1\lambda + b_2\lambda^2 + b_3\lambda^3 + b_4\lambda^4 \quad [29]$$

with

$$b_0 = -0.005\ 62, \quad b_1 = 0.0146, \quad b_2 = 0.0685, \quad b_3 = -0.0115 \\ b_4 = -0.0115, \quad b_4 = 5.60 \times 10^{-4} \quad [30]$$

The largest standard error in this case was found to be SE = 0.0312, with an error estimate for the fitting of

$$a|_{\text{error}} = a_{80\text{C}} \pm \text{SE} \quad [31]$$

We now have the data available to plot the conductivity as a function of the water content at 30 and 80°C. We use the fitted sorption data at 80°C in our fitting of the BFCM at 70°C.

### Fitting Conductivity at 30°C

The conductivity fit of Sone et al. (Eq. 25) was modified to plot the conductivity as a function of water content by using Eq. 26. This range of activity values was used to determine the range in which the conductivity data may lie by substituting Eq. 28 into Eq. 25. It should be stressed that this error estimate only accounts for the error in fitting the sorption isotherm data and does not include experimental errors associated with the measurements of conductivity vs water vapor activity. However, since any fit that lies within this error estimate would fall well within any estimate of the total error, a fit to this data is considered satisfactory.

The determination of parameter values for an optimum fit must be constrained by physical considerations. Examining the conductivity data in Fig. 1, it is clear that  $\lambda_{\text{min}}$  should lie somewhere between 1.5 and 2, since this is the approximate range where the conductivity bounds intersect the  $x$  axis.

The (noneffective) diffusion coefficient  $D_{12}$ , which is assumed not to vary with water content, is used to normalize the other diffusion coefficients. Introducing proportionality constants and using relation 24, we get

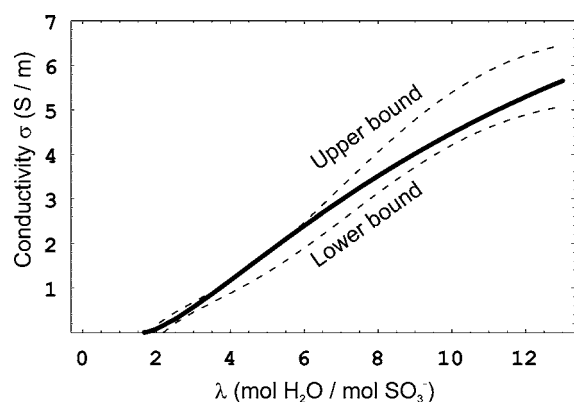


**Figure 1.** BFCM and anticipated upper and lower bounds on conductivity resulting from expected error in fit to sorption isotherm data at 30°C.

$$D_{1M} = D_{12}A_1\lambda^s \text{ and } D_{2M} = D_{12}A_2\lambda^s \quad [32]$$

where  $A_1$ ,  $A_2$ ,  $s$ , and the magnitude of  $D_{12}$  can be set to obtain a fit that lies within the upper and lower bounds on conductivity. The suitability of the fit can be quantified using the relative error of the conductivity fit relative to the experimental curve of Sone et al.

$$\% \text{ error} = 100 \left( \frac{\sigma_{\text{Sone}} - \sigma}{\sigma_{\text{Sone}}} \right) \quad [33]$$

This relative error was used as a guide to maintain the error within reasonable bounds while ensuring a fit within the range of conductivity values defined by the standard error in the sorption isotherms, and the resulting parameter values are

$$\lambda_{\min} = 1.65 \quad [34]$$

$$D_{12} = 6.5 \times 10^{-9} \text{ m}^2 \text{ s}^{-1} \quad [35]$$

$$s = 0.83 \quad [36]$$

$$A_1 = 0.084 \quad [37]$$

and

$$A_2 = 0.5 \quad [38]$$

The minimum water content  $\lambda_{\min}$  was chosen such that the model conductivity threshold closely matches the data of Sone et al. A reasonable order of magnitude for  $D_{12}$  was chosen from a literature survey, and  $A_1$ ,  $A_2$ ,  $s$ , and  $D_{12}$  were then varied such that the BFCM results lay within the error bounds for all  $\lambda$ .

Next, we performed a sensitivity analysis and found that the conductivity was most sensitive to changes in the values of  $A_1$  and  $s$ . As an additional measure in assessing the fit to experimental data, contours of the maximum absolute error between the experimental conductivity data and our model were plotted over the entire range of water contents, as parameters  $A_1$  and  $s$  were varied. As shown in Fig. 2, the above  $A_1$  value was found to yield the lowest absolute error over the entire range of water contents for an  $s$  value of 1.25. Figure 1 shows the fit of the BFCM to the experimental data, using the value of  $s = 0.8$ , and the corresponding relative errors are shown in Fig. 3.

The coefficients  $A_1$  and  $A_2$  reflect the relative size of  $D_{1M}$  and  $D_{2M}$ , respectively. Since the fitted value of  $A_1$  is much smaller than  $A_2$ , this implies that the resistance of the membrane to hydronium diffusion is much larger than to water. Given that hydronium ions have a net charge while water has no net charge, this is reasonable because we expect the interaction forces between the membrane (with charged sulfonate heads) and the hydronium ions to be stronger than the forces between membrane and water.

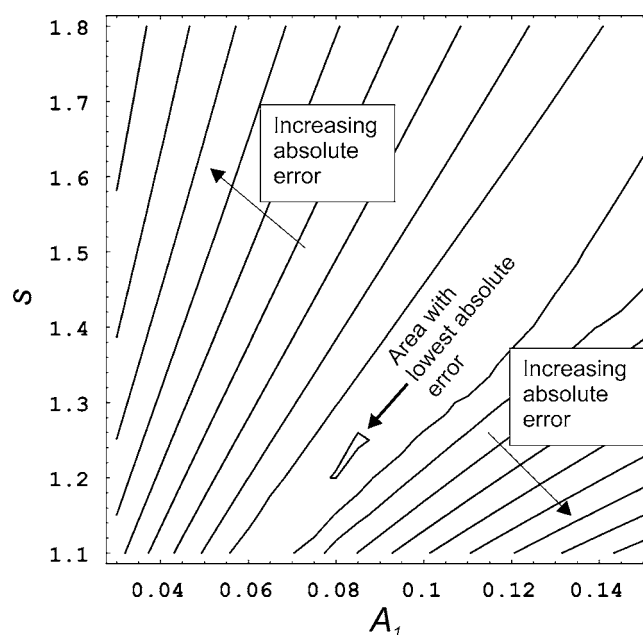


**Figure 2.** Contour plot of maximum relative error over the entire range of water contents, comparing BFCM to Ref. 5, for various  $A_1$  and  $s$  values. Error is with respect to median value between experimental bounds.

Examination of the relative error in Fig. 3 shows the error is less than 10% over a wide range of  $\lambda$  values. The plot of our conductivity curve in Fig. 1 fits within the anticipated range of conductivity values over almost the entire range of water contents, with the fit falling slightly outside the error bounds at a water content of approximately 5. At lower water contents ( $\lambda$  of about 2), the relative error is amplified by the small conductivity values, but the absolute error is in fact small.

*Analyzing magnitude of parameters.*—Though we have used several constraints in fitting the parameters to the experimental data, it is beyond the scope of this work to perform a systematic analysis of the parameters involved. However, to verify that the obtained diffusion coefficients  $D_{12}$ ,  $D_{1M}$ , and  $D_{2M}$  are reasonable, we have varied the parameter  $D_{12}$  by an order of magnitude (larger and smaller) and then selected  $A_1$  and  $A_2$  values for the best possible fit to the conductivity data of Sone at 30°C.

Decreasing  $D_{12}$  by an order of magnitude to  $6.5 \times 10^{-10} \text{ m}^2 \text{ s}^{-1}$  yields  $A_1$  and  $A_2$  values of 1.2 and 10, respectively, while increasing  $D_{12}$  to  $6.5 \times 10^{-8} \text{ m}^2 \text{ s}^{-1}$  results in values of  $A_1$  and  $A_2$  of 0.007 and 0.05, respectively. Figure 4 shows the predicted

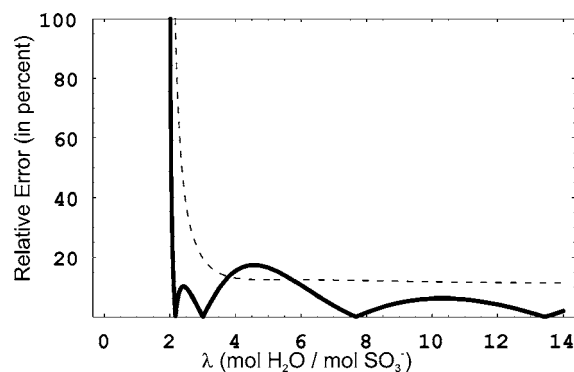


**Figure 3.** Relative error in conductivity: BFCM (solid) compared to relative error due to error in fit to experimental data (dashed).

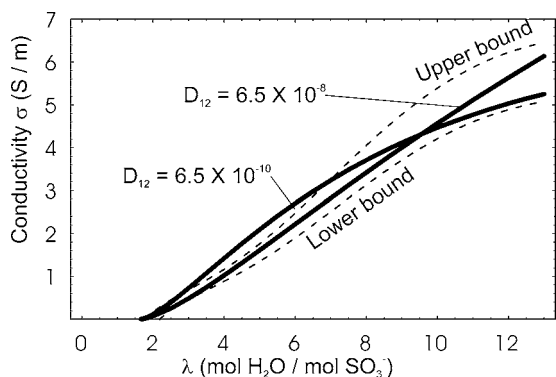


**Figure 4.** BFCM conductivity (solid) for  $D_{12} = 6.5 \times 10^{-10} \text{ m}^2 \text{ s}^{-1}$ , and  $D_{12} = 6.5 \times 10^{-8} \text{ m}^2 \text{ s}^{-1}$  compared to expected range of conductivity values (dashed).

conductivity curves for both cases. From Fig. 1 and 4 we note that the larger  $D_{12}$  value provides a significantly better fit; this suggests that  $D_{12}$  should be at least on the order of  $10^{-9} \text{ m}^2 \text{ s}^{-1}$ . For  $D_{12} = 6.5 \times 10^{-8} \text{ m}^2 \text{ s}^{-1}$  the curve in Fig. 4 lies closer to the center of the error bounds than that for  $D_{12} = 6.5 \times 10^{-9} \text{ m}^2 \text{ s}^{-1}$ .

To support the choice of a  $D_{12}$  value of  $6.5 \times 10^{-9} \text{ m}^2 \text{ s}^{-1}$ , we first note that any fit lying entirely within the error bounds obtained from the analysis of the sorption isotherm data is considered satisfactory. Second, a proton diffusivity value of  $4.5 \times 10^{-9} \text{ m}^2 \text{ s}^{-1}$  was reported in conjunction with the Nernst-Planck equation.<sup>8</sup> Considering that the latter is in fact a simplification of the Stefan-Maxwell equations in the limit of the solute species (in this case protons) being infinitely diluted by the solvent (in this case water), the Nernst-Planck diffusivity is in fact equivalent to a Stefan-Maxwell diffusion coefficient. The  $D_{12}$  value of  $6.5 \times 10^{-9} \text{ m}^2 \text{ s}^{-1}$  is of the same order of magnitude and is a better choice in terms of fit.

A further point is that, regardless of the order of magnitude of  $D_{12}$ , we found that the ratio of the values of  $D_{1M}$  and  $D_{2M}$  that provides for reasonable fits was of the same order of magnitude. The fact that the ratio of the values for the diffusion coefficients remains relatively similar is encouraging in terms of the generality of the model and serves to reinforce the suitability of the selected values for the parameters  $A_1$  and  $A_2$ .

#### Comparison with other Conductivity Models

Both Springer et al.<sup>5</sup> and Thampan et al.<sup>2</sup> have presented conductivity expressions for Nafion 117 membranes. Springer et al.'s model is the result of an empirical curve fit of the form

$$\sigma_{\text{Springer}} = \exp \left[ 1268 \left( \frac{1}{303} - \frac{1}{273 + T_{\text{cell}}} \right) \right] \sigma_{30} \quad [39]$$

where  $T_{\text{cell}}$  is the cell temperature in degrees centigrade and  $\sigma_{30}$  is the conductivity (with units of  $\text{S cm}^{-1}$ ) at  $30^\circ\text{C}$  that is measured to be a linear function of  $\lambda$

$$\sigma_{30} = 0.005139\lambda - 0.00326(\lambda > 1) \quad [40]$$

At this point we should note that Springer et al. omit whether the membrane considered was in the *E* form or some heat-treated form. We will assume that it is for the *E* form and use it for comparison purposes.

Thampan's conductivity expression is developed from a theoretical model related to the BFCM presented here, but is based on the dusty fluid model formulation.<sup>1</sup> This model takes the form<sup>2</sup>

$$\sigma_{\text{Thampan}} = (\varepsilon - \varepsilon_0)^q \left( \frac{\lambda_1^0}{1 + \delta} \right) c_{\text{HA},0} \alpha \quad [41]$$

Note that  $\alpha$  is the degree of dissociation,  $c_{\text{HA},0}$  is the acid group concentration in the pore fluid,  $\delta$  is the ratio  $D_{12}/D_{1M}$ , and  $\lambda_1^0$  is the

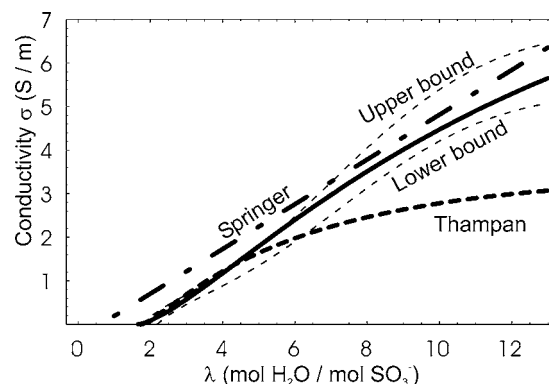


**Figure 5.** Comparison of calculated conductivity using BFCM (solid) and models of Springer et al. (Ref. 5) and Thampan et al. (Ref. 2) against experimental data of Sone et al. (Ref. 4) for *E*-form Nafion 117 at  $30^\circ\text{C}$ .

equivalent conductance of hydronium at infinite dilution. Note also the presence of the Bruggeman correction.

The conductivity models of Ref. 2 and 5 are compared to our model in Fig. 5, which also shows the expected range of the data. Springer's model falls within the upper and lower bounds on conductivity given by the estimate of the error in sorption data for high water contents  $\lambda$ , but not for low values of  $\lambda$ . Thampan's model falls within the upper and lower bounds for low water contents; however, for higher water contents, the model deviates significantly from the experimental results.

The error relative to the curve fit of Sone et al. is plotted in Fig. 6 for our model and those of Springer et al. and Thampan et al. Springer et al.'s fit to the conductivity data is good at higher water contents only, while Thampan et al.'s model provides a good fit at lower water contents only. The proposed BFCM provides a good fit throughout the range, and lower relative errors for virtually the entire range of  $\lambda$ .

#### Fitting Conductivity at $70^\circ\text{C}$

The only BFCM parameters assumed to depend on temperature are the diffusion coefficients, because the complementary model for calculating the fraction of dissociated sulfonate heads  $\alpha$  already includes temperature dependence, and the minimum water content  $\lambda_{\text{min}}$  is not expected to be temperature dependent. For simplicity, the same functional dependence on temperature was assumed for all diffusion coefficients, and we used a fitting procedure similar to the one used for  $30^\circ\text{C}$ . We used the data of Sone for  $70^\circ\text{C}$  with the sorption isotherm data for  $80^\circ\text{C}$  to obtain a plot of the conductivity as a function of water content at  $70^\circ\text{C}$ .

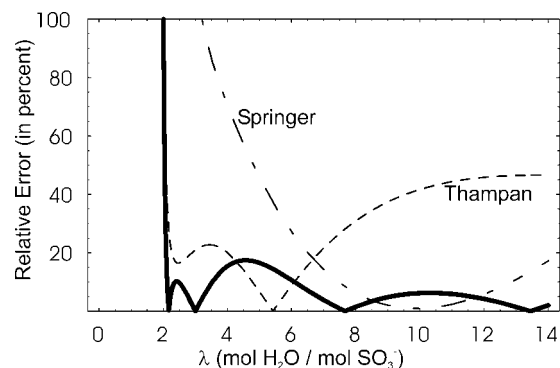


**Figure 6.** Relative error in calculated conductivities using BFCM (solid) and models of Springer et al. (Ref. 5) and Thampan et al. (Ref. 2) relative to experimental results (Ref. 4) at  $30^\circ\text{C}$ .

For brevity, a direct comparison of the BFCM to the results using Thampan and Springer models at 70°C is not presented here, but we note that Springer et al.'s model is markedly inferior to that at 30°C, with a minimum relative error of approximately 20% and lying outside the upper bound of conductivity range at all water contents. There are a number of possible causes: we may not be comparing their expression to data for Nafion of the correct form ( $E$ ,  $N$ , or  $S$ ); their temperature dependence is incorrect; or there may be experimental errors in the conductivity measurements. Thampan et al.'s model fit at higher water contents is adequate for  $\lambda < 5$ , but poor at higher water contents (approximately 20% error and outside the expected conductivity range). Again, the BFCM has lower overall error almost throughout the range of water contents. With the fitted parameters available at two temperatures, we can proceed with predictions at intermediate temperatures.

### Predicting Conductivity at 45°C

*Temperature dependence of parameters.*—The reference diffusion coefficient (which we set to be  $D_{12}$ ) varies with temperature

$$D_{12}(30^\circ\text{C}) = 6.5 \times 10^{-9} \text{ m}^2 \text{ s}^{-1} \quad [42]$$

and

$$D_{12}(70^\circ\text{C}) = 1.30 \times 10^{-8} \text{ m}^2 \text{ s}^{-1} \quad [43]$$

Assuming that all the diffusion coefficients vary in the same way, and that the variation is of Arrhenius type, we used our data points to determine an activation energy ( $E_a$ ), which is assumed to apply for all  $\lambda$ . Thus

$$D_{12}(T) = 6.5 \times 10^{-9} \left\{ \exp \left[ \frac{E_a}{R} \left( \frac{1}{303 \text{ K}} - \frac{1}{T} \right) \right] \right\} \text{ m}^2 \text{ s}^{-1} \quad [44]$$

with  $E_a/R = 1800 \text{ K}$ . We note that the conductivity in Springer's model is also assumed to vary with an Arrhenius law with activation energy of  $E_a/R = 1268 \text{ K}$ .

*Sorption isotherm.*—In order to gauge the ability of the BFCM to correctly predict the temperature dependence of conductivity, we decided to compare our theoretical curve to Sone's data at 45°C. One problem in attempting this is lack of reliable sorption isotherm data at temperatures near 45°C. For example, data<sup>9</sup> for 50°C is suspect because it implies that more water is sorbed by a membrane at 50°C than at 25°C. This is contrary to the expected decrease in amount of water sorbed as temperature increases.<sup>10</sup> Rather than using these data, we implemented the chemical model of Weber and Newman developed for determining  $\lambda$  for a vapor-equilibrated membrane<sup>10</sup> and used it to provide sorption isotherm data, and then in conjunction with Sone's data at 45°C to plot conductivity as a function of the number of sorbed waters. A standard error of  $\pm 0.038$  was used on the activity (the same standard error as was used at 30°C) to provide error bars within which conductivity is expected to lie.

As a check on Weber and Newman's chemical model for sorption, we used their chemical model to translate the conductivity data of Sone from a function of activity to a function of water content at 30, 70, and 80°C. For the case of 30°C, Weber and Newman's conversion and the conversion using the fit to data overlap in the mid-to-high water content range. At lower water contents, the differences between the sorption isotherm model and the fit to the data for low water contents become more significant. In the conversion process for 70 and 80°C, a significant overlap was noted for both temperatures over the entire range of water contents. We concluded that the effect of a 10°C temperature variation on the sorption isotherms is small, and that using the sorption data at 80°C to convert the conductivity data at 70°C is acceptable. Weber and Newman's chemical model appears to provide a reasonable enough translation of the conductivity data, and should provide a useful basis to validate the temperature dependence behavior of our model.

*Comparison to conductivity data.*—Figure 7 compares the BFCM, and the models of Springer et al. and Thampan et al., to the

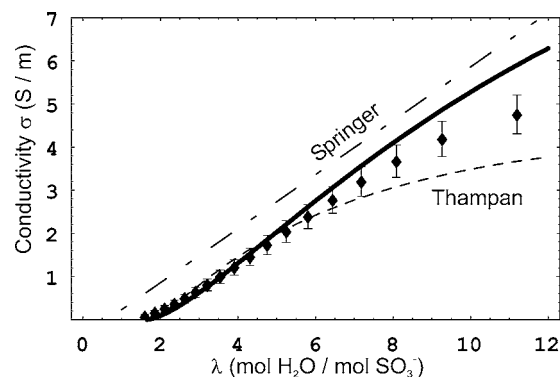


Figure 7. Prediction of membrane conductivity at 45°C with BFCM and models of Springer et al. (Ref. 5) and Thampan et al. (Ref. 2).

data at 45°C. Springer's model falls outside the error across the range, while Thampan's provides the best fit at very low water contents. Although the BFCM falls outside the error bounds at high and low water contents, it generally provides a better fit over a broader range of water contents.

The higher errors at high and low water content have to be considered in light of the fact that we are not using experimental data for sorption isotherm plots, but rather, in the absence of reliable data, a chemical model. Though this chemical model has been shown to generally agree with available data,<sup>10</sup> it has not been validated at or near 45°C. In addition, small deviations between the sorption isotherm model and experimental data, which would normally be perfectly acceptable, can introduce potentially large errors in the conductivity predictions. Consider that a standard error of  $\pm 0.038$  at an activity near 1 ( $\pm 3.8\%$  variation) can cause the conductivity to range between approximately 5.2 and 4.4  $\text{S m}^{-1}$  ( $\pm 8\%$  variation in conductivity approximately) at a water content of around 11. This illustrates the significant effect that relatively small errors in sorption isotherm models (or data) can have on the determination of conductivity as a function of  $\lambda$ .

The good agreement of the BFCM predictions with experimental data over a broad range of water contents suggests that the temperature dependence of conductivity is well represented. A more rigorous analysis of the temperature dependence requires additional experimental data. Ideally, sorption isotherm data and conductivity data, allowing for the determination of conductivity as a function of water content, should be obtained for a wider range of temperatures to allow for a more systematic analysis. In fairness, and without detracting from the features of the present model, it should be noted that the predictive abilities of the classical models of Springer et al. and Thampan et al. might also benefit from accounting for temperature dependence in the sorption isotherms.

### A Guide for Future Work: Necessary Parameters for Conductivity Model Implementation

In closing, it is useful to summarize what information is required, either from experiments or fundamental simulations, in order to apply the BFCM and the more general BFM2 to other membranes, and provide guidance for further experimental investigations of membranes. We start with the fundamental properties of the membrane and transport phenomena.

Application of the model requires specification of the EW and the dry density of the membrane, or the molar volume (required for the porosity portion of the model). The model requires knowledge of which species are involved in the transport within the membrane (e.g., water, hydronium). The model also requires specification of the fraction of dissociated acidic heads forming the charge carrying species (required for the counting portion of the model). Such information could be obtained experimentally or from a complementary dissociation model.

The specification of the BFCM parameters (i.e.,  $\lambda_{\min}$ ,  $D_{12}$ ,  $s$ ,  $A_1$ , and  $A_2$ ) requires, at a minimum, conductivity data as a function of water content for a range of temperatures. The most convenient data presentation for use with the BFCM, or any other model for that matter, is conductivity data measured as a function of water content for a range of temperatures. This would allow for direct fitting to the data, without requiring an exhaustive search for sorption isotherms. If conductivity data are obtained as a function of activity, then sorption isotherm data for the same type of membrane and with the same pretreatment should also be documented. Other relevant empirical data required for the general BFM2 are water diffusion coefficient through the membrane, and the electro-osmotic drag coefficient.

In addition to treating the parameters as fitting parameters, it might be possible to devise experiments or molecular dynamics models which can directly provide insight into some of these parameters. Such simulations could, for example, elucidate the interaction forces between species, thus shedding more light on the  $D_{12}$ ,  $D_{1M}$ , and  $D_{2M}$  parameters (and thus  $A_1$ ,  $A_2$ , and  $s$ ). Finally, documenting of  $\lambda_{\min}$  for each membrane, the water content below which conductivity falls below some critical level and thus becomes effectively zero, is also required.

### Conclusion

In this paper we developed a transport model for polymer electrolyte membranes based on the binary friction model. We investigated the driving forces in the binary friction model and found that the pressure gradient terms were negligible compared to the other driving force terms. This BFM2 transport model was cast in a general form to allow for broad applicability and tailoring to suit other types of PFSA membranes. As a tool for investigating the unknown parameters in the general BFM2, a simplified binary friction conductivity model (BFCM) was derived to represent conditions found in ac impedance conductivity measurements and to allow predictions of conductivity as a function of water content and temperature.

In order to compare the BFCM predictions with experimental results, we first applied the model to I100 EW Nafion. We first used available conductivity and sorption data at 30°C to determine the parameters of the conductivity model ( $\lambda_{\min}$ ,  $D_{12}$ ,  $s$ ,  $A_1$ , and  $A_2$ ). We also fit the conductivity data at 70°C and, assuming that all diffusion coefficients had the same Arrhenius-type temperature dependence, determined the activation energy. We then used this to predict the conductivity at 45°C and established that this temperature dependence allowed us to provide a very satisfactory fit to the data. Compared to the other established membrane models, the proposed BFCM model was shown to provide a more consistent fit to the data over the entire range of water contents and at different temperatures.

While the focus of the model performance assessment was on Nafion 1100 equivalent weight (EW), the binary friction membrane transport model is quite general and should be applicable to other PFSA membranes. This is supported by preliminary results in applying the model to Dow membranes and membrane C, whereby rational changes in a single model parameter based on physical considerations of structural differences from Nafion yield conductivity predictions that are in good agreement with experimental measurements.<sup>11</sup> More detailed information and data on other membranes are required to rigorously assess the model's ability to predict the behavior of a variety of different membranes.

One of the inherent advantages of the simplified BFCM is the ability to gain insight into the necessary transport parameters from fitting the conductivity data, and an important feature is that the subset of transport coefficients in the BFCM is the same as in the general BFM2. Thus, with additional data on water transport parameters in specific membranes (water diffusion coefficient and electro-osmotic drag), the BFM2 and all its required parameters can be fully specified and the general model applied to account for coupled proton and water transport.

Table IV. Species present within the membrane.

Subscript	Species
1	Protonated complex
2	Free waters
W	Total sorbed waters
fw	Fixed waters
pw	Waters in protonated complex
sh	Sulfonate heads
M	Membrane

### Acknowledgments

Dr. David Harrington provided valuable comments and suggestions during the course of this work. This research was funded in part by grants to N.D. from the Natural Sciences and Engineering Research Council of Canada and the MITACS Network of Centres of Excellence.

University of Victoria assisted in meeting the publication costs of this article.

### Appendix

#### Counting of Species Involved in Transport

The expressions for mole fractions  $X_i$ , mole densities  $c_i$ , and porosity  $\varepsilon$  for use in the transport model are derived in this appendix. We start by assuming that we have a proton forming a complex with a number of waters residing within the water sorbed by a membrane. A protonated water complex consists of  $\omega_{pw}$  waters and one extra proton. In order to simplify our analysis, we assume that at all times the protons are accompanied by the same water molecule(s) in the protonated complex.<sup>1,12</sup> In effect, we are neglecting any contribution of the so-called Grotthuss hopping mechanism to transport, as the inclusion of such a mechanism is beyond the scope of this work and would significantly complicate the model. Furthermore, we recall that the presence of the membrane reduces the effectiveness of the Grotthuss mechanism.<sup>13</sup>

In addition to the protonated complexes we have water and membrane backbone. The water and protonated complexes form one phase, the membrane backbone another. We recall from Part I<sup>1</sup> that  $\lambda$  is defined as the number of water molecules sorbed by the membrane per sulfonate head, while  $\alpha$  represents the fraction of the sulfonate heads which have dissociated, allowing their protons to combine with waters sorbed by the membrane to form protonated complexes ( $0 \leq \alpha \leq 1$ ). It follows that  $\omega_{pw}\alpha$  water molecules per sulfonate head have been converted into protonated complexes. For generality, the parameter  $\omega_{pw}$  could be retained in the model. However, when considering transport within vapor-equilibrated Nafion, it is reasonable to assume that hydronium is the protonated complex that is formed. Therefore, we assume that  $\omega_{pw} = 1$  throughout. Referring to Table IV for definitions of the subscripts used in this counting exercise, the total number of sorbed waters is, due to the definition of  $\lambda$ ,  $n_w = \lambda n_{sh}$ , i.e., the number of sulfonate heads is

$$n_{sh} = \frac{n_w}{\lambda} \quad [A-1]$$

Due to electroneutrality, the number of protons available to dissociate into the membrane pore fluid must be equal to the number of sulfonate heads

$$n_1 = \alpha n_{sh} = \frac{\alpha}{\lambda} n_w \quad [A-2]$$

We can also introduce a parameter  $\gamma$  as the number of fixed waters per sulfonate head. These are waters that are so strongly bound to the sulfonate heads that they effectively become part of the membrane phase, and do not contribute to transport. The number of fixed waters is then given as

$$n_{fw} = \gamma n_{sh} = \frac{\gamma}{\lambda} n_w \quad [A-3]$$

However, since we were able to fit the model in all cases with  $\gamma = 0$ , we choose to drop it from the model. The total number of waters sorbed by the membrane is the sum of the free waters, fixed waters, and waters associated with protonated complexes  $n_w = n_2 + n_{fw} + \omega_{pw}n_1$ . Therefore, using  $\gamma = 0$  and  $\omega_{pw} = 1$ , we have

$$n_2 = n_w \left( \frac{\lambda - \alpha}{\lambda} \right) \quad [A-4]$$

Having counted the numbers of all the species present, we now determine the molar densities, which involve partial molar volumes. We could not find data on the exact partial molar volume of hydronium or other protonated complexes under the given conditions, i.e., within a hydrated membrane. In order to be able to progress, we make the reasonable assumption that the partial molar volume of water and hydronium is approximately the same.

Indeed, the addition of an extra proton to bulk water causes the hydrogen bonds to be contracted, and although a proton is added, a volume contraction is measured. In



fact, the partial molar volume for an individual  $H^+$  ion is  $-5.4 \text{ cm}^3 \text{ mol}^{-1}$ , indicative of this volume contraction.<sup>4,14</sup> Based on this observation, we shall assume that, even though the hydronium ion has an additional hydrogen atom, it has the same partial molar volume as water. We also assume that the partial molar volume of a protonated complex is approximately equal to the number of waters in the complex times the partial molar volume of water,  $\bar{V}_1 \cong \omega_{pw} \bar{V}_2 = \bar{V}_2$ , which implicitly involves assuming that the molar volumes add to give the molar volume of the complex.

Ideally, we should use partial molar volumes in this counting exercise, since we are dealing with a solution (water and hydronium ions), and the volumes of the species involved (membrane, water, and protons) will not necessarily add as the membrane sorbs water. However, since the water and membranes form a two-phase system (thus we would expect the volume of membrane and water after sorption to be reasonably close to the sum of the volumes of water and membrane before sorption), and we were unable to find information on the partial molar volumes for a such a system, we assume that the molar volumes of the species are equal to the partial molar volumes. From here on in our analysis we replace partial molar volumes  $\bar{V}$  with molar volumes  $V_M$ .

The volume occupied by the free waters is

$$V_2 = V_{M,2} n_2 = V_{M,2} n_w \left( \frac{\lambda - \alpha}{\lambda} \right) \quad [\text{A-5}]$$

and the volume occupied by the protonated complex is

$$V_1 = V_{M,2} n_1 = V_{M,2} n_w \frac{\alpha}{\lambda} \quad [\text{A-6}]$$

The volume occupied by the fixed waters is zero, and finally the volume occupied by the membrane is

$$V_M = V_{M,M} n_{sh} = V_{M,M} n_w \frac{1}{\lambda} \quad [\text{A-7}]$$

where  $V_{M,M}$  is the volume of membrane per mole of acid heads ( $V_{M,M} = EW/\rho_{dry}$ , where  $\rho_{dry}$  is the dry density of the polymer membrane).

We recall that the membrane forms a two-phase system with the sulfonate heads at the interface between the liquid and membrane phases, Ref. 1. We assume that the pore fluid consists of only the free waters and the protonated complexes. The fixed waters and the membrane are assumed to be separate from the pore fluid phase, and are thus excluded from the total pore fluid volume.

The total volume of pore fluid is, from Eq. A-5 and A-6

$$V_p = V_1 + V_2 = V_{M,2} n_w \quad [\text{A-8}]$$

The mole density of protonated complexes within the pore fluid is  $c_1 = n_1/V_p = (1/V_{M,2})(\alpha/\lambda)$  and the mole density of free waters within the membrane is  $c_2 = n_2/V_p = (1/V_{M,2})(\lambda-\alpha)/\lambda$ . The total mole density of the pore fluid is

$$c_t = c_1 + c_2 = \frac{1}{V_{M,2}} \quad [\text{A-9}]$$

We can now calculate the mole fraction for the protonated complexes

$$X_1 = \frac{c_1}{c_t} = \frac{\alpha}{\lambda} \quad [\text{A-10}]$$

and the mole fraction of free waters

$$X_2 = \frac{c_2}{c_t} = \frac{\lambda - \alpha}{\lambda} \quad [\text{A-11}]$$

The porosity is defined as the volume of the pore fluid divided by the total volume,  $\varepsilon = V_p/V_t$ , and since the total volume is the sum of all the volumes that make up the system

$$V_t = V_1 + V_2 + V_M = n_w \left( V_{M,2} + \frac{V_{M,M}}{\lambda} \right) \quad [\text{A-12}]$$

the porosity can be written as

$$\varepsilon = \frac{\lambda}{\lambda + V_{M,M}/V_{M,2}} \quad [\text{A-13}]$$

## List of Symbols

$A_1, A_2$	model fitting parameters, 1
$a$	activity of species $i$ , 1
$c$	molar density, $\text{mol m}^{-3}$
$D_i$	diffusion coefficient (Nernst-Planck equation), $\text{m}^2 \text{ s}^{-1}$
$D_{ij}^{S-M}$	Stefan-Maxwell diffusion coefficient, $\text{m}^2 \text{ s}^{-1}$
$D_{M,M}^+$	membrane diffusion coefficient, $\text{m}^2 \text{ s}^{-1}$
$E_a$	activation energy, J $\text{mol}^{-1}$
$E_\eta$	activation energy for viscosity of water, J $\text{mol}^{-1}$
EW	equivalent weight, g $\text{mol}^{-1}$
$\Delta H^0$	enthalpy change for proton solvation, J $\text{mol}^{-1}$
$N, N$	molar flux relative to fixed reference frame, $\text{mol m}^{-2} \text{ s}^{-1}$
$M$	molar mass, kg $\text{m}^{-3}$
$n$	Number of moles of a species (within the Appendix), 1
$p$	pressure, Pa
$q$	Bruggeman exponent, 1
$s$	diffusion coefficient exponent, 1
SE	standard error, 1

$T$	temperature, K
$T_{cell}$	cell temperature (Springer's model), $^\circ\text{C}$
$\bar{V}$	partial molar volume, $\text{m}^3 \text{ mol}^{-1}$
$V_M$	molar volume, $\text{m}^3 \text{ mol}^{-1}$
$V$	volume, $\text{m}^3$
$\hat{v}$	nondimensional molar volume, 1
$X$	mole fraction, 1
$x$	relative humidity, 1
$z$	charge number, 1

## Greek

$\alpha$	degree of dissociation of acidic heads, 1
$\beta$	dimensionless parameter, 1
$\gamma$	number of waters fixed to sulfonate head (not participating in transport), 1
$\gamma_i$	activity coefficient for species $i$ , 1
$\delta$	ratio of mutual to membrane effective diffusion coefficients, 1
$\varepsilon$	porosity, 1
$\varepsilon_0$	threshold porosity, 1
$\eta$	viscosity, kg $\text{m}^{-1} \text{ s}^{-1}$
$\Theta$	dimensionless parameter, 1
$\lambda$	number of waters sorbed per acid head, 1
$\lambda_i^0$	equivalent conductance for species $i$ at infinite dilution, S $\text{m}^2 \text{ mol}^{-1}$
$\mu$	chemical potential, J $\text{mol}^{-1}$
$\mu^e$	electrochemical potential, J $\text{mol}^{-1}$
$\rho_{dry}$	dry membrane density, kg $\text{m}^{-3}$
$\sigma$	conductivity, S $\text{m}^{-1}$
$\Phi$	potential, V
$\phi$	volume fraction, 1
$\omega_{pw}$	number of waters within hydrated proton complex, 1

## Constants

$R$	universal gas constant 8.314 J $\text{mol}^{-1} \text{ K}^{-1}$
$F$	Faraday's constant 96 485 C $\text{mol}^{-1}$
$k_B$	Boltzmann's constant $1.3807 \times 10^{-23}$ J $\text{K}^{-1}$

## Subscripts

f	fixed species in membrane
fw	fixed waters
i	species I
M	membrane or a phase within the membrane
min	minimum
p	pore
pw	waters in protonated complex
ref	reference quantity
sat	corresponding to saturated vapor conditions
sh	sulfonate heads
t	total
W	total sorbed waters
w	water
1	protonated complex (typically hydronium ion)
2	Waters participating in transport

## Superscripts

o	standard state
visc	viscous

## References

- J. Fimrite, H. Struchtrup and N. Djilali, *J. Electrochem. Soc.*, **152**, A1804 (2005).
- P. J. A. M. Kerkhof, *Chem. Eng. J.*, **64**, 319 (1996).
- T. Thampan, S. Malhotra, H. Tang, and R. Datta, *J. Electrochem. Soc.*, **147**, 3242 (2000).
- Y. Sone, P. Ekdunge, and D. Simonsson, *J. Electrochem. Soc.*, **143**, 1254 (1996).
- T. E. Springer, T. A. Zawodzinski, and S. Gottesfeld, *J. Electrochem. Soc.*, **138**, 2334 (1991).
- R. Taylor and R. Krishna, *Multicomponent Mass Transfer*, John Wiley & Sons, Toronto (1993).
- J. T. Hinatsu, M. Mizuhata, and H. Takenaka, *J. Electrochem. Soc.*, **141**, 1493 (1994).
- M. Verbrugge and R. F. Hill, *J. Electrochem. Soc.*, **137**, 1131 (1990).
- D. R. Morris and X. Sun, *J. Appl. Polym. Sci.*, **50**, 1445 (1993).
- A. Z. Weber and J. Newman, *J. Electrochem. Soc.*, **151**, A311 (2004).
- J. Fimrite, Transport Phenomena in Polymer Electrolyte Membranes, MASC Thesis, University of Victoria (2004).
- P. Berg, K. Promislow, J. St-Pierre, J. Stumper, and B. Wetton, *J. Electrochem. Soc.*, **151**, A341 (2004).
- K. D. Kreuer, *Chem. Mater.*, **8**, 610 (1996).
- B. E. Conway, *Ionic Hydration In Chemistry and Biophysics*, Elsevier Scientific Publishing Company, Amsterdam (1981).